

## CAUSTIC REGION FIELDS OF A 3D CASSEGRAIN SYSTEM PLACED IN BI-ISOTROPIC HOMOGENEOUS CHIRAL MEDIUM

Arshad, M. Q. Mehmood\*, and M . J. Mughal

Faculty of Electronic Engineering, GIK Institute of Engineering Sciences and Technology, Topi, Swabi 23640, KPK, Pakistan

**Abstract**—This paper presents the electromagnetic field expressions for 3D cassegrain system embedded in a bi-isotropic chiral medium. Mathematical formulation of Maslov is used to find the field expressions in the focal region. Effect of chirality (both the weak and strong) on focal region fields is analyzed. It is seen that when the chirality effect is weak (i.e.,  $\kappa < 1$ ), chiral medium will support positive phase velocity (PPV) for both the left circularly polarized (LCP) and the right circularly polarized (RCP) modes. However for strong chiral medium (i.e.,  $\kappa > 1$ ), one mode travels with PPV and the other mode travels with negative phase velocity (NPV). The line plots are given to show the behavior of fields in the focal plane of 3D cassegrain system by changing the chirality parameter ( $\kappa$ ).

### 1. INTRODUCTION

An object is chiral if it can not be superimposed on its mirror image neither by translation nor by rotation. A chiral object has the property of handedness, it must be either left or right handed object. Interaction between the electromagnetic wave and the chiral objects results in rotation of the polarization of wave to the right or left depending on handedness of the object. Uniform distribution and random orientation of such handed objects form a homogeneous composite medium, which is known as a chiral medium [1]. Different reflectors are placed in chiral medium due to its unique characteristics over an ordinary medium like polarization control, impedance matching and cross coupling of electric and magnetic fields. Desirable values of the wave impedance and the propagation constants can be obtained by changing the permittivity

---

*Received 8 August 2011, Accepted 25 August 2011, Scheduled 2 September 2011*

\* Corresponding author: Muhammad Qasim Mehmood (qasim145ps@gmail.com).

( $\epsilon$ ), permeability ( $\mu$ ) and chirality parameter ( $\kappa$ ) of the chiral media. Hence, a chiral medium gives more freedom to adjust (decrease or increase) the reflection and transmission, because it can be controlled by variation of three parameters ( $\epsilon$ ,  $\mu$  and  $\kappa$ ) instead of two parameters ( $\epsilon$  and  $\mu$ ) as in the case of achiral medium [2–4]. Moreover, a negative refractive index can be realized in a magnetoelectrically chiral medium with few restrictions. When the chirality parameter is greater than the square root of the product of permittivity and permeability, the backward wave will occur at one of the two circularly polarized eigenwaves [5, 6]. Realizing the unique characteristics of chiral medium, we have embedded the 3D Cassegrain system in chiral medium in this problem. Two different cases are considered depending upon the effect of chirality parameter on the wave propagation in chiral media. In the first case, chiral medium supports PPV for both the LCP and RCP modes. In the second case, chiral medium supporting PPV for one mode and NPV for the other mode is taken into account. Maslov's method is used to study the fields in the focal region. It combines the simplicity of asymptotic ray theory and the generality of the Fourier transform method [7, 8]. Maslov's method has been utilized by many authors to study different focusing systems in the caustic region [10–19]. Focusing system in this problem is three dimensional Cassegrain system which is embedded inside a chiral medium. Division of the present paper is as under:

In Section 2, reflection of plane wave from perfect electric conductor (PEC) placed in chiral medium is discussed. Section 3 is about the receiving characteristics of three dimensional Cassegrain system placed in chiral medium for both  $\kappa < 1$  and  $\kappa > 1$ . In Section 4, results and discussions are given and Section 5 is about the conclusion.

## 2. REFLECTION OF PLANE WAVE FROM PERFECT ELECTRIC CONDUCTOR (PEC) PLACED IN CHIRAL MEDIUM

Reflection phenomena of plane waves from PEC plane placed in chiral medium is discussed in [9]. We recapitulate it here to present it in a form suitable for our present work. Consider reflection of RCP wave from PEC plane lying along  $xz$ -plane as shown in Figure 1. An RCP wave traveling with phase velocity  $\omega/kn_2$  and unit amplitude is incident on the plane making angle  $\alpha$  with  $z$ -axis. Reflected wave is composed of two waves with opposite handedness. An LCP wave is reflected making an angle  $\alpha_1 = [\sin^{-1}(n_2/n_1 \sin \alpha)]$  and with amplitude  $2 \cos \alpha / (\cos \alpha + \cos \alpha_1)$ . The phase velocity of LCP wave is  $\omega/kn_1$ . An RCP wave is reflected making angle  $\alpha$  and amplitude

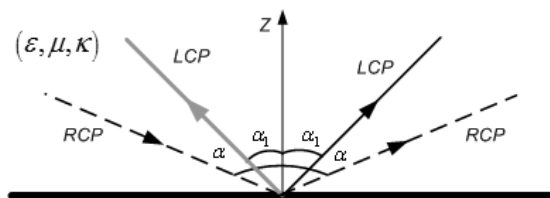


**Figure 1.** Reflection of RCP wave from PEC plane [3].

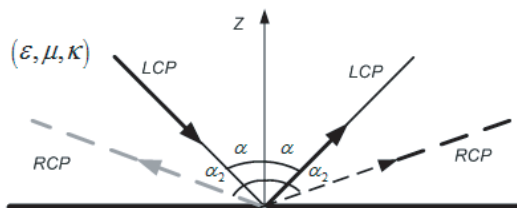


**Figure 2.** Reflection of LCP wave from PEC plane [3].

$(\cos \alpha - \cos \alpha_1)/(\cos \alpha + \cos \alpha_1)$ . If we take  $\kappa < 1$ , then  $n_1 > n_2$  and  $\alpha_1 < \alpha$ , i.e., LCP wave bends towards normal, because it is traveling slower than RCP wave. For  $\kappa > 1$ ,  $\alpha_1$  is negative and the wave is reflected in the wrong way, it may be called negative reflection (shown as gray in Figure 1). This means that for  $\kappa > 1$ , LCP reflected wave sees the chiral medium as NPV medium. Similarly when an LCP wave with unit amplitude is incident on PEC plane making angle  $\alpha$  with  $z$ -axis, as shown in Figure 2, we get two reflected waves of opposite handedness. An RCP wave is reflected at angle  $\alpha_2 = [\sin^{-1}(n_1/n_2 \sin \alpha)]$  with amplitude  $2 \cos \alpha / (\cos \alpha + \cos \alpha_2)$  and an LCP wave at angle  $\alpha$  and amplitude  $(\cos \alpha - \cos \alpha_2) / (\cos \alpha + \cos \alpha_2)$ . If we take  $\kappa < 1$ , then  $n_1 > n_2$  and  $\alpha_2 > \alpha$ . If  $\kappa = 0$  then only normal reflection take place, and if  $\kappa$  increases the difference between the angle  $\alpha$  and  $\alpha_1, \alpha_2$  increases. For  $\kappa > 1$ , we have negative reflection for RCP reflected wave (shown as gray in Figure 2) [17].

### 3. GEOMETRICAL OPTICS FIELDS OF THREE DIMENSIONAL CASSEGRAIN SYSTEM PLACED IN CHIRAL MEDIUM

Cassegrain system consists of two reflectors, one is paraboloidal main reflector and other is hyperboloidal subreflector as shown in Figure 3.

In this problem we are considering the receiving characteristics of 3D Cassegrain system. When both RCP and LCP waves are incident on the main paraboloidal reflector, it cause four reflected waves designated as LL, RR, LR and RL [17]. These four waves are then incident on the secondary hyperboloidal subreflector and will cause eight reflected waves designated as LLL, RRR, LLR, RRL, RLR, RLL, LRR and LRL. Only four waves(LLL, RRR, LLR, RRL) will converge in the focal region while other four waves (RLR, RLL, LRR, LRL) will diverge. In this paper we are considering only four converging rays after reflection from hyperboloidal subreflector as shown in Figure 4. For  $\kappa > 1$ ,  $n_1 = \frac{1}{1-\kappa} < 0$  and  $n_2 = \frac{1}{1+\kappa} > 0$ , so LCP wave travels with NPV and RCP wave with PPV. For  $\kappa < -1$  RCP wave travels with NPV and LCP wave with PPV. We have depicted here the case of  $\kappa > 1$  only because for  $\kappa < -1$ , we can get the solutions from  $\kappa > 1$  by interchanging the role of LCP and RCP modes [18]. Cassegrain system for  $\kappa > 1$  is shown in Figure 5. LLL and RRR rays are reflected at the same angle while RRL and LLR rays have different response. It can be seen that only two rays (LLL and RRR) are contributing to the focus, while RRL and LLR rays are divergent. Equations for paraboloidal and hyperboloidal reflector of Cassegrain system are given by

$$\zeta_1 = \frac{\rho_1^2}{4f} - f + c, \quad \zeta_2 = \frac{a}{b} [\rho_2^2 + b^2]^{1/2}, \quad c^2 = a^2 + b^2 \quad (1)$$

where

$$c^2 = a^2 + b^2, \quad \rho_1^2 = \xi_1^2 + \eta_1^2, \quad \rho_2^2 = \xi_2^2 + \eta_2^2, \quad aR_2 = c\zeta_2 - a^2 \quad (2)$$

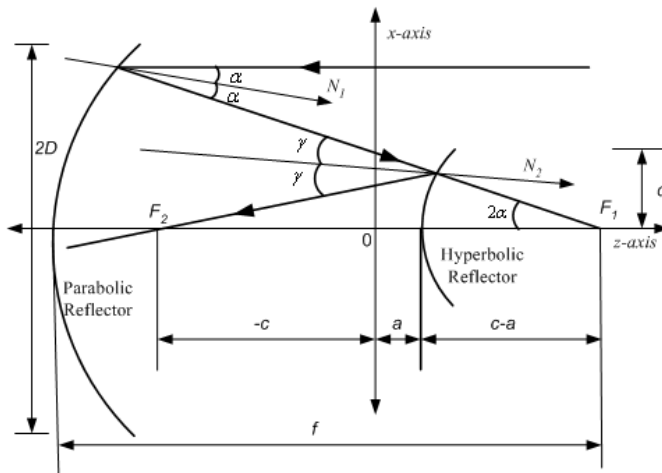


Figure 3. Three dimensional Cassegrain system.

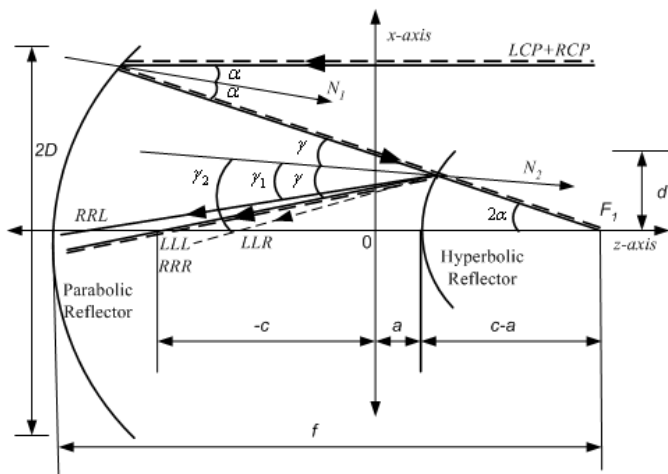


Figure 4. 3D Cassegrain system in chiral medium for  $\kappa < 1$ .

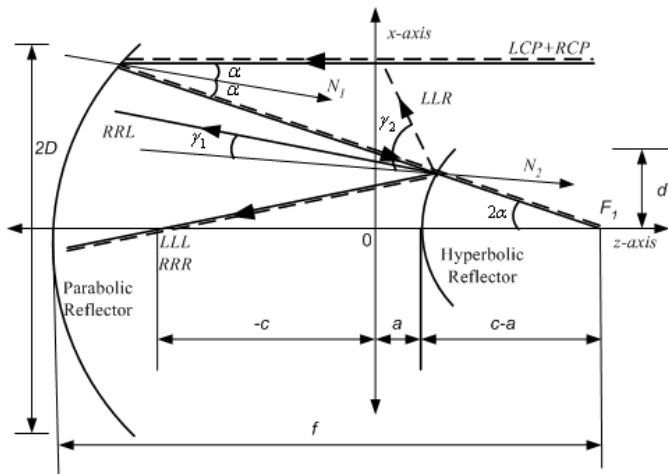


Figure 5. 3D cassegrain system in chiral medium for  $\kappa > 1$ .

and  $(\xi_1, \eta_1, \zeta_1)$  and  $(\xi_2, \eta_2, \zeta_2)$  are the cartesian coordinates of the points on the paraboloidal and hyperboloidal reflectors, respectively. Unit vectors normal to the paraboloidal and hyperboloidal surfaces are as following, respectively

$$\mathbf{N}_1 = \sin \alpha \cos \beta \mathbf{a}_x + \sin \alpha \sin \beta \mathbf{a}_y - \cos \alpha \mathbf{a}_z \quad (3a)$$

$$\mathbf{N}_2 = -\sin \psi \cos \beta \mathbf{a}_x - \sin \psi \sin \beta \mathbf{a}_y + \cos \psi \mathbf{a}_z \quad (3b)$$

where

$$\sin \alpha = \frac{\rho_1}{\sqrt{\rho_1^2 + 4f^2}}, \quad \cos \alpha = \frac{2f}{\sqrt{\rho_1^2 + 4f^2}}, \quad \tan \beta = \frac{\eta_1}{\xi_1} \quad (4a)$$

$$\sin \psi = -\frac{a\rho_2}{b\sqrt{R_1 R_2}}, \quad \cos \psi = \frac{b\zeta_2}{a\sqrt{R_1 R_2}}, \quad \tan \beta = \frac{\eta_2}{\xi_2} \quad (4b)$$

while  $R_1$  and  $R_2$  are the distances from the point  $(\xi_2, \eta_2, \zeta_2)$  on the hyperboloidal reflector to the caustic points  $z = c$  and  $z = -c$ , respectively. Incident waves on main paraboloidal reflector having unit amplitude are given by.

$$Q_L = \exp(jkn_1z), \quad Q_R = \exp(jkn_2z) \quad (5)$$

Consider the case of normal incidence such that these waves are incident at an angle  $\alpha$  with surface normal  $\mathbf{N}_1$  as shown in Figure 3 to Figure 5. The reflected wave vectors will be LL, RR, RL and LR as given in [12]. We will take two, RR and LL, waves that will incident on hyperboloidal subreflector and converge as well after reflection. The wave vectors of these (LLL, RRR, RRL and LLR) reflected waves by the hyperboloidal subreflector are given as

$$\begin{aligned} \mathbf{P}_{LLL} = & -n_1 \sin(2\alpha - 2\psi) \cos \beta \mathbf{a}_x - n_1 \sin(2\alpha - 2\psi) \sin \beta \mathbf{a}_y \\ & - n_1 \cos(2\alpha - 2\psi) \mathbf{a}_z \end{aligned} \quad (6a)$$

$$\begin{aligned} \mathbf{P}_{RRR} = & -n_2 \sin(2\alpha - 2\psi) \cos \beta \mathbf{a}_x - n_2 \sin(2\alpha - 2\psi) \sin \beta \mathbf{a}_y \\ & - n_2 \cos(2\alpha - 2\psi) \mathbf{a}_z \end{aligned} \quad (6b)$$

$$\begin{aligned} \mathbf{P}_{RRL} = & -n_1 \sin(\gamma_1 - \psi) \cos \beta \mathbf{a}_x - n_1 \sin(\gamma_1 - \psi) \sin \beta \mathbf{a}_y \\ & - n_1 \cos(\gamma_1 - \psi) \mathbf{a}_z \end{aligned} \quad (6c)$$

$$\begin{aligned} \mathbf{P}_{LLR} = & -n_2 \sin(\gamma_2 - \psi) \cos \beta \mathbf{a}_x - n_2 \sin(\gamma_2 - \psi) \sin \beta \mathbf{a}_y \\ & - n_2 \cos(\gamma_2 - \psi) \mathbf{a}_z \end{aligned} \quad (6d)$$

The initial amplitudes for these four reflected rays are

$$A_{0LLL} = \left( \frac{\cos \alpha - \cos \alpha_2}{\cos \alpha + \cos \alpha_2} \right) \left( \frac{\cos \gamma - \cos \gamma_2}{\cos \gamma + \cos \gamma_2} \right) \quad (7a)$$

$$A_{0RRR} = \left( \frac{\cos \alpha - \cos \alpha_1}{\cos \alpha + \cos \alpha_1} \right) \left( \frac{\cos \gamma - \cos \gamma_1}{\cos \gamma + \cos \gamma_1} \right) \quad (7b)$$

$$A_{0RRL} = \left( \frac{\cos \alpha - \cos \alpha_1}{\cos \alpha + \cos \alpha_1} \right) \left( \frac{2 \cos \gamma}{\cos \gamma + \cos \gamma_1} \right) \quad (7c)$$

$$A_{0LLR} = \left( \frac{\cos \alpha - \cos \alpha_2}{\cos \alpha + \cos \alpha_2} \right) \left( \frac{2 \cos \gamma}{\cos \gamma + \cos \gamma_2} \right) \quad (7d)$$

And the corresponding initial phases are

$$S_{0LLL} = -n_1\zeta_1 = n_1 \left[ 2f \frac{\cos 2\alpha}{1 + \cos 2\alpha} - c \right] \quad (8a)$$

$$S_{0RRR} = -n_2\zeta_1 = n_2 \left[ 2f \frac{\cos 2\alpha}{1 + \cos 2\alpha} - c \right] \quad (8b)$$

$$S_{0RRL} = -n_2\zeta_1 = n_2 \left[ 2f \frac{\cos 2\alpha}{1 + \cos 2\alpha} - c \right] \quad (8c)$$

$$S_{0LLR} = -n_1\zeta_1 = n_1 \left[ 2f \frac{\cos 2\alpha}{1 + \cos 2\alpha} - c \right] \quad (8d)$$

In the above equations  $R_1$  and  $R_2$  are the distances from the point  $(\xi_2, \eta_2, \zeta_2)$  to the focal points  $z = -c$  and  $z = c$ , respectively with  $c^2 = a^2 + b^2$ . The cartesian coordinates of the rays reflected by the hyperboloidal subreflector are given by.

$$x_{LLL} = \xi_2 + P_{xLLL}t, \quad x_{RRR} = \xi_2 + P_{xRRR}t \quad (9a)$$

$$x_{RRL} = \xi_2 + P_{xRRL}t, \quad x_{LLR} = \xi_2 + P_{xLLR}t \quad (9b)$$

$$y_{LLL} = \eta_2 + P_{yLLL}t, \quad y_{RRR} = \eta_2 + P_{yRRR}t \quad (9c)$$

$$y_{RRL} = \eta_2 + P_{yRRL}t, \quad y_{LLR} = \eta_2 + P_{yLLR}t \quad (9d)$$

$$z_{LLL} = \zeta_2 + P_{zLLL}t, \quad z_{RRR} = \zeta_2 + P_{zRRR}t \quad (9e)$$

$$z_{RRL} = \zeta_2 + P_{zRRL}t, \quad z_{LLR} = \zeta_2 + P_{zLLR}t \quad (9f)$$

where

$$t_1 = \sqrt{(\xi_2 - \xi_1)^2 + (\eta_2 - \eta_1)^2 + (\zeta_2 - \zeta_1)^2} \quad (10a)$$

$$t = \sqrt{(x - \xi_2)^2 + (y - \eta_2)^2 + (z - \zeta_2)^2} \quad (10b)$$

The Jacobian transformation of reflected rays can be found using  $\left[ J(t) = \frac{D(t)}{D(0)} \right]$ . The GO field for each ray can now be written as

$$U(r)_{LLL} = A_{0LLL} [J_{LLL}]^{-1/2} \exp [-jk (S_{0LLL} + n_1^2 t + n_1 t_1)] \quad (11a)$$

$$U(r)_{RRR} = A_{0RRR} [J_{RRR}]^{-1/2} \exp [-jk (S_{0RRR} + n_2^2 t + n_2 t_1)] \quad (11b)$$

$$U(r)_{RRL} = A_{0RRL} [J_{RRL}]^{-1/2} \exp [-jk (S_{0RRL} + n_1^2 t + n_1 t_1)] \quad (11c)$$

$$U(r)_{LLR} = A_{0LLR} [J_{LLR}]^{-1/2} \exp [-jk (S_{0LLR} + n_2^2 t + n_2 t_1)] \quad (11d)$$

where  $A_0$  and  $S_0$  are the initial amplitudes and phases respectively. Their expressions are given in Eqs. (7)–(14). The phase functions are given by

$$\begin{aligned} S_{LLL} &= S_{0LLL} + n_1 t_1 + n_1^2 t - x_{LLL} P_{xLLL} - y_{LLL} P_{yLLL} \\ &\quad + x P_{xLLL} + y P_{yLLL} \end{aligned} \quad (12a)$$

$$\begin{aligned} S_{RRR} &= S_{0RRR} + n_2 t_1 + n_2^2 t - x_{RRR} P_{xRRR} - y_{RRR} P_{yRRR} \\ &\quad + x P_{xRRR} + y P_{yRRR} \end{aligned} \quad (12b)$$

$$\begin{aligned} S_{RRL} &= S_{0RRL} + n_1 t_1 + n_1^2 t - x_{RRL} P_{xRRL} - y_{RRL} P_{yRRL} \\ &\quad + x P_{xRRL} + y P_{yRRL} \end{aligned} \quad (12c)$$

$$\begin{aligned} S_{LLR} &= S_{0LLR} + n_2 t_1 + n_2^2 t - x_{LLR} P_{xLLR} - y_{LLR} P_{yLLR} \\ &\quad + x P_{xLLR} + y P_{yLLR} \end{aligned} \quad (12d)$$

In these phase functions  $S_0$  and  $t_1$  are given above. While the extra terms are given by

$$\begin{aligned} S_{exLLL} &= n_1^2 t - x_{LLL} P_{xLLL} - y_{LLL} P_{yLLL} + x P_{xLLL} + y P_{yLLL} \\ &= n_1^2 t - (\xi_2 + P_{xLLL} t) P_{xLLL} + (\eta_2 + P_{yLLL} t) P_{yLLL} \\ &\quad + x P_{xLLL} + y P_{yLLL} \\ &= (P_{zLLL})^2 t + (x - \xi_2) P_{xLLL} + (y - \eta_2) P_{yLLL} \\ &= (x - \xi_2) P_{xLLL} + (y - \eta_2) P_{yLLL} + (z - \zeta_2) P_{zLLL} \\ &= -n_1 x \sin(2\alpha - 2\psi) \cos \beta - n_1 y \sin(2\alpha - 2\psi) \sin \beta \\ &\quad - n_1 z \cos(2\alpha - 2\psi) + n_1 \xi_2 \sin(2\alpha - 2\psi) \cos \beta \\ &\quad + n_1 \eta_2 \sin(2\alpha - 2\psi) \sin \beta + n_1 \zeta_2 \cos(2\alpha - 2\psi) \end{aligned} \quad (13)$$

Similarly

$$\begin{aligned} S_{exRRR} &= -n_2 x \sin(2\alpha - 2\psi) \cos \beta - n_2 y \sin(2\alpha - 2\psi) \sin \beta \\ &\quad - n_2 z \cos(2\alpha - 2\psi) + n_2 \xi_2 \sin(2\alpha - 2\psi) \cos \beta \\ &\quad + n_2 \eta_2 \sin(2\alpha - 2\psi) \sin \beta + n_2 \zeta_2 \cos(2\alpha - 2\psi) \end{aligned} \quad (14)$$

$$\begin{aligned} S_{exRRL} &= -n_1 x \sin(\gamma_1 - \psi) \cos \beta - n_1 y \sin(\gamma_1 - \psi) \sin \beta \\ &\quad - n_1 z \cos(\gamma_1 - \psi) + n_1 \xi_2 \sin(\gamma_1 - \psi) \cos \beta \\ &\quad + n_1 \eta_2 \sin(\gamma_1 - \psi) \sin \beta + n_1 \zeta_2 \cos(\gamma_1 - \psi) \end{aligned} \quad (15)$$

$$\begin{aligned}
 S_{exLLR} = & -n_2x \sin(\gamma_2 - \psi) \cos \beta - n_2y \sin(\gamma_2 - \psi) \sin \beta \\
 & -n_2z \cos(\gamma_2 - \psi) + n_2\xi_2 \sin(\gamma_2 - \psi) \cos \beta \\
 & +n_2\eta_2 \sin(\gamma_2 - \psi) \sin \beta + \zeta_2 \cos(\gamma_2 - \psi)
 \end{aligned} \tag{16}$$

Since GO becomes infinite at caustic region, so we found approximate field at the caustic by Maslov’s method. To calculate the field at caustic region we need expression  $\left[ J(t) \frac{\partial(P_x, P_y)}{\partial(x, y)} \right]$  for all four rays, reflected from hyperboloidal subreflector, which are given below.

$$\left[ J(t)_{LLL} \frac{\partial(P_{xLLL}, P_{yLLL})}{\partial(x, y)} \right] = \frac{n_1 \Gamma_\zeta \sin(2\alpha - 2\psi) \cos^2(2\alpha - 2\psi) \cos(\psi)}{R_2^2 \cos^2(\alpha) \cos(2\alpha - \psi) \Gamma_\xi \Gamma_\eta} \tag{17a}$$

$$\left[ J(t)_{RRR} \frac{\partial(P_{xRRR}, P_{yRRR})}{\partial(x, y)} \right] = \frac{n_2 \Gamma_\zeta \sin(2\alpha - 2\psi) \cos^2(2\alpha - 2\psi) \cos(\psi)}{R_2^2 \cos^2(\alpha) \cos(2\alpha - \psi) \Gamma_\xi \Gamma_\eta} \tag{17b}$$

$$\begin{aligned}
 \left[ J(t)_{LLR} \frac{\partial(P_{xLLR}, P_{yLLR})}{\partial(x, y)} \right] = & \frac{n_2 \sin(\gamma_2 - \psi) \cos^2(\gamma_2 - \psi) \cos(\psi)}{R_2^2 \cos^2(\alpha) \cos(\gamma_2) \Gamma_\xi \Gamma_\eta} \\
 & \times \left[ \frac{n_1 \cos(\gamma)}{\sqrt{n_2^2 - n_1^2 \cos(\gamma)}} [1 - \Gamma_{\zeta_1}] - \Gamma_{\zeta_1} \right]
 \end{aligned} \tag{17c}$$

$$\begin{aligned}
 \left[ J(t)_{RRL} \frac{\partial(P_{xRRL}, P_{yRRL})}{\partial(x, y)} \right] = & \frac{n_1 \sin(\gamma_1 - \psi) \cos^2(\gamma_1 - \psi) \cos(\psi)}{R_2^2 \cos^2(\alpha) \cos(\gamma_1) \Gamma_\xi \Gamma_\eta} \\
 & \times \left[ \frac{n_2 \cos(\gamma)}{\sqrt{n_1^2 - n_2^2 \cos(\gamma)}} [1 - \Gamma_{\zeta_1}] - \Gamma_{\zeta_1} \right]
 \end{aligned} \tag{17d}$$

where

$$\Gamma_\zeta = 1 - \frac{2ac}{R_1(R_2 + a)} [\Gamma_\xi \cos^2 \beta + \Gamma_\eta \sin^2 \beta] \tag{18a}$$

$$\Gamma_\xi = \frac{1 + \tan(2\alpha) \tan(\alpha) \cos^2(\beta)}{1 + \tan(2\alpha) \tan(\psi) \cos^2(\beta)} \tag{18b}$$

$$\Gamma_\eta = \frac{1 + \tan(2\alpha) \tan(\alpha) \sin^2(\beta)}{1 + \tan(2\alpha) \tan(\psi) \sin^2(\beta)} \tag{18c}$$

$$\Gamma_{\zeta_1} = \frac{ac}{R_1(R_2 + a)} [\Gamma_\xi \cos^2 \beta + \Gamma_\eta \sin^2 \beta] \tag{18d}$$

After substituting all the required parameters and simplifying them we will get the following final expressions at caustic region.

$$\begin{aligned}
 U(r)_{\text{LLL}} &= \frac{jk}{2\pi} \left[ \int_{A_1}^{A_2} + \int_{-A_2}^{-A_1} \right] \int_0^{2\pi} A_{0\text{LLL}}(\xi) \frac{R_2^3 \cos^3(\alpha) \sin(4\alpha)}{f^2} \\
 &\quad \times \left[ \frac{n_1^3 \sin(2\alpha - 2\psi) \cos(2\alpha - \psi)}{2 \cos \psi} \Gamma_\xi \Gamma_\eta \Gamma_\zeta \right]^{1/2} \\
 &\quad \times \exp[-jk\{S_{0\text{LLL}} + n_1 t_1 + S_{ex\text{LLL}}\}] d(\alpha) d(\beta) \quad (19a)
 \end{aligned}$$

$$\begin{aligned}
 U(r)_{\text{RRR}} &= \frac{jk}{2\pi} \left[ \int_{A_1}^{A_2} + \int_{-A_2}^{-A_1} \right] \int_0^{2\pi} A_{0\text{RRR}}(\xi) \frac{R_2^3 \cos^3(\alpha) \sin(4\alpha)}{f^2} \\
 &\quad \times \left[ \frac{n_2^3 \sin(2\alpha - 2\psi) \cos(2\alpha - \psi)}{2 \cos \psi} \Gamma_\xi \Gamma_\eta \Gamma_\zeta \right]^{1/2} \\
 &\quad \times \exp[-jk\{S_{0\text{RRR}} + n_2 t_1 + S_{ex\text{RRR}}\}] d(\alpha) d(\beta) \quad (19b)
 \end{aligned}$$

$$\begin{aligned}
 U(r)_{\text{RRL}} &= \frac{jk}{2\pi} \left[ \int_{A_1}^{A_2} + \int_{-A_1}^{-A_2} \right] \int_0^{2\pi} A_{0\text{RRL}}(\xi) \frac{R_2^3 \cos^3(\alpha) \sin(4\alpha) \Gamma_\zeta}{2f^2} \\
 &\quad \times \left[ \frac{n_1^3 \sin(\gamma_1 - \psi) \cos(\gamma_1) \Gamma_\xi \Gamma_\eta}{\cos(\psi)} \right]^{1/2} \\
 &\quad \times \left[ \frac{n_2 \cos(\gamma) \Gamma_{\zeta_1}}{\sqrt{n_1^2 - n_2^2 \sin^2(\gamma)}} + \Gamma_{\zeta_1-1} \right]^{-1/2} \\
 &\quad \times \exp[-jk\{S_{0\text{RRL}} + n_1 t_1 + S_{ex\text{RRL}}\}] d(\alpha) d(\beta) \quad (19c)
 \end{aligned}$$

$$\begin{aligned}
 U(r)_{\text{LLR}} &= \frac{jk}{2\pi} \left[ \int_{A_1}^{A_2} + \int_{-A_1}^{-A_2} \right] \int_0^{2\pi} A_{0\text{LLR}}(\xi) \frac{R_2^3 \cos^3(\alpha) \sin(4\alpha) \Gamma_\zeta}{2f^2} \\
 &\quad \times \left[ \frac{n_2^3 \sin(\gamma_2 - \psi) \cos(\gamma_2) \Gamma_\xi \Gamma_\eta}{\cos(\psi)} \right]^{1/2} \\
 &\quad \times \left[ \frac{n_1 \cos(\gamma) \Gamma_{\zeta_1}}{\sqrt{n_2^2 - n_1^2 \sin^2(\gamma)}} + \Gamma_{\zeta_1-1} \right]^{-1/2} \\
 &\quad \times \exp[-jk\{S_{\text{LLR}} + n_2 t_1 + S_{ex\text{LLR}}\}] d(\alpha) d(\beta) \quad (19d)
 \end{aligned}$$

#### 4. RESULTS AND DISCUSSIONS

Field pattern around the caustic of a Cassegrain system are determined using Eqs. (19a)–(19d) by using Maslov's method. Values for different

parameters of Cassegrain system are:  $kf = 25$ ,  $ka = 8$ ,  $kb = 9$ ,  $kd = 6$ ,  $kD = 18$ . Limits of integration for Eqs. (19a)–(19d) are selected using the following relations [19].

$$A_1 = 2 \tan^{-1} \left( \frac{D}{2f} \right), \quad A_2 = \tan^{-1} \left( \frac{d}{2c} \right) \quad (20)$$

Equations of caustic for LLL and RRR rays are given by Eq. (19a) and Eq. (19b). These are similar as in the case of ordinary medium [19]. LLL and RRR rays coincide for all values of  $\kappa$ . As the value of  $\kappa$  increases, magnitude of the field at caustic increases. This behavior is depicted in Figures 6 and 7. For  $\kappa = 0$ ,  $n_1 = n_2 = 1$  and

$$U_{LLL} = U_{RRR} = 0 \quad (21)$$

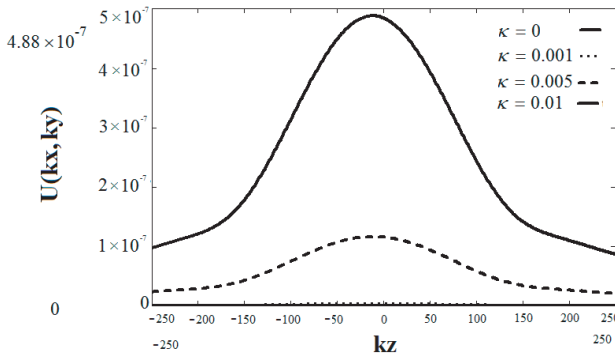


**Figure 6.**  $|U_{LLL}|$  of 3D Cassegrain system at  $kx = 0$ ,  $ky = 0$ , for  $\kappa = 0, 0.001, 0.005, 0.01$ .

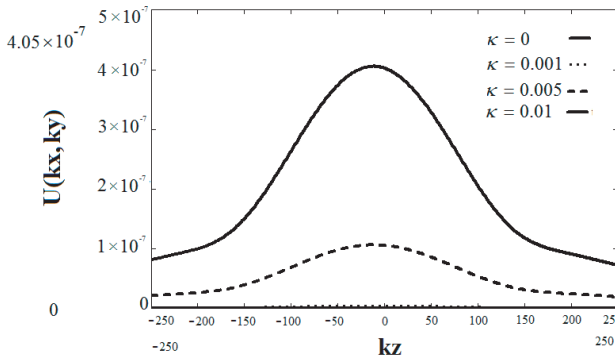


**Figure 7.**  $|U_{RRR}|$  of 3D Cassegrain system at  $kx = 0$ ,  $ky = 0$ , for  $\kappa = 0, 0.001, 0.005, 0.01$ .

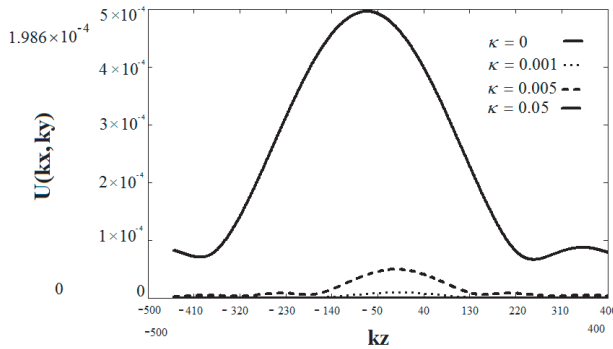


**Figure 8.**  $|U_{\text{RRL}}|$  of 3D cassegrain system at  $kx = 0$ ,  $ky = 0$ , for  $\kappa = 0, 0.001, 0.005, 0.01$ .

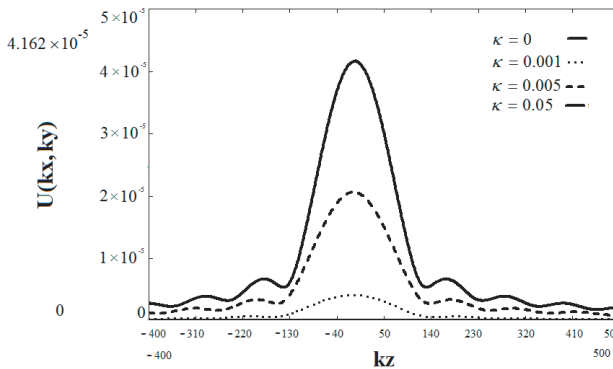


**Figure 9.**  $|U_{\text{LLR}}|$  of 3D Cassegrain system at  $kx = 0$ ,  $ky = 0$ , for  $\kappa = 0, 0.001, 0.005, 0.01$ .

Equations of caustic for RRL and LLR rays are given by Eq. (19c) and Eq. (19d). As the value of  $\kappa$  increases, gap between the focal points of RRL and LLR rays increases as shown in Figures 8 and 9. It is due to the fact that enlarging the value of chirality parameter causes reduction in the phase velocity of LLR ray, i.e., it slows down. While by increasing the value of  $\kappa$ , phase velocity of RRL ray increases. This is why the gap between RRL and LLR rays continues to increase with increase in the value of  $\kappa$  as shown in Figure 9. For  $\kappa = 0$ ,  $n_1 = n_2 = 1$  and

$$U_{\text{RRL}} = U_{\text{LLR}} = 0 \quad (22)$$

Equations (21) and (22) explains that for zero chirality parameter,  $\alpha_1 = \alpha$  and  $\alpha_2 = \alpha$ , i.e., LL and RR rays reduce to zero amplitude. Since LLL, RRR, LLR and RRL rays are reflected as the result of

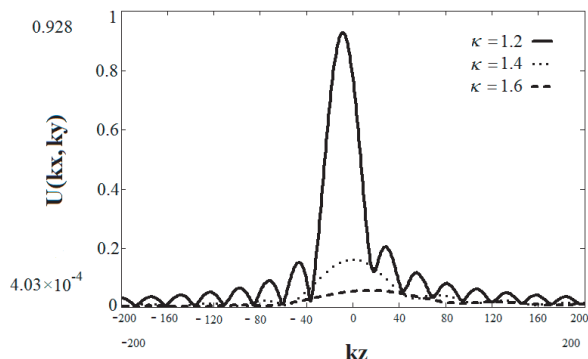


**Figure 10.**  $|U_{LLL}|$  of 3D Cassegrain system at  $kx = 0, ky = 0$ , for  $\kappa = 1.2, 1.4, 1.6$ .

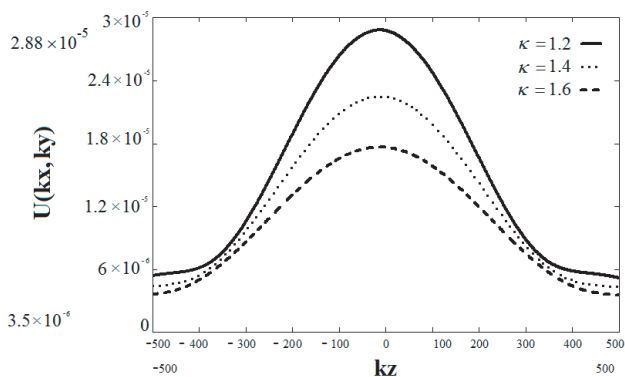


**Figure 11.**  $|U_{RRR}|$  of 3D Cassegrain system at  $kx = 0, ky = 0$ , for  $\kappa = 1.2, 1.4, 1.6$ .

incidence of LL and RR rays on hyperboloidal reflector. So it is quite obvious that if LL and RR rays vanishes at  $\kappa = 0$  then LLL, RRR, RRL and LLR rays also have zero amplitude for zero chirality as shown in Figures 6–11. While other four rays LRL, LRR, RLR, RRL, caused due the incidence of RL and LR will be like ordinary medium waves [19] for zero chirality case. Due to these properties, it can be advantageous in RF absorber and reflection controlling applications.

Plots of LLL and RRR rays for  $\kappa > 1$  are given in Figures 10 and 11, respectively. In this case LCP wave is traveling with NPV and RCP with PPV. Due to this, LLL and RRR rays are located at same location as in the case of ordinary medium, while RRL and LLR waves diverge out and do not form a real focus. Hence for  $\kappa > 1$ , negative reflections occur which can be applicable where invisibility is required.

## 5. CONCLUSION

It is found that excitation of a Cassegrain system placed in chiral medium by the plane wave yield eight rays four of them converge and their field expressions are determined in this paper. LLL and RRR, rays are focused at the same location as if the system is placed in an ordinary medium [19]. It is also found that for weak chirality parameter case other two rays, LLR and RRL, are focused on the opposite sides of the caustic region locating in an ordinary medium [19]. As  $\kappa$  increases, gap between the focal points of LLR and RRL rays increases. For NPV case, it is observed that caustic for LLL and RRR rays does not change, while the caustics of LLR and RRL rays disappear because these two rays are now diverging.

## REFERENCES

1. Zouhdi, S., A. Sihvola, and A. P. Vinogradov, *Metamaterials and Plasmonics: Fundamentals, Modelling, Applications*, Springer, 2008.
2. Mehmood, M. Q., M. J. Mughal, and T. Rahim, "Focal region fields of Gregorian system placed in homogeneous chiral medium," *Progress In Electromagnetics Research M*, Vol. 11, 241–256, 2010.
3. Mehmood, M. Q. and M. J. Mughal, "Analysis of focal region fields of PEMC Gregorian system embeded in homogeneous chiral medium," *Progress In Electromagnetics Research Letters*, Vol. 18, 155–163, 2010.
4. Mehmood, M. Q., M. J. Mughal, and T. Rahim, "Focal region fields of Cassegrain system placed in homogeneous chiral medium," *Progress In Electromagnetics Research B*, Vol. 21, 329–346, 2010.
5. Dong, W. T., L. Gao, and C. W. Qiu, "Goos-Hänchen shift at the surface of chiral negative refractive media," *Progress In Electromagnetics Research*, Vol. 90, 255–268, 2009.
6. Qiu, C. W., H. Y. Yao, L. W. Li, S. Zouhdi, and T. S. Yeo, "Backward waves in magnetoelectrically chiral media: Propagation, impedance, and negative refraction," *Physical Review B*, Vol. 75, 155120, 2007.
7. Maslov, V. P., "Perturbation theory and asymptotic methods," Izdat. Moskov. Gos. Univ., Moscow, 1965 (in Russian).
8. Maslov, V. P. and V. E. Nazaikinski, "Asymptotics of operator and pseudo-differential equations," *Consultants Bureau*, N.Y., 1988.

9. Lakhtakia, A., V. V. Varadan, and V. K. Varadan, "What happens to plane waves at the planar interfaces of mirror conjugated chiral media," *Journal of the Optical Society of America A: Optics, Image Science, and Vision*, Vol. 6, No. 1, 2326, January 1989.
10. Rahim, T., M. J. Mughal, Q. A. Naqvi, and M. Faryad, "Paraboloidal reflector in chiral medium supporting simultaneously positive phase velocity and negative phase velocity," *Progress In Electromagnetics Research*, Vol. 92, 223–234, 2009.
11. Ghaffar, A., Q. A. Naqvi, and K. Hongo, "Analysis of the fields in three dimensional Cassegrain system," *Progress In Electromagnetics Research*, Vol. 72, 215–240, 2007.
12. Rahim, T., M. J. Mughal, M. Faryad, and Q. A. Naqvi, "Fields around the focal region of a paraboloidal reflector placed in isotropic chiral medium," *Progress In Electromagnetics Research B*, Vol. 15, 57–76, 2009.
13. Rahim, T., M. J. Mughal, M. Faryad, and Q. A. Naqvi, "Focal region field of a paraboloidal reflector coated with isotropic chiral medium," *Progress In Electromagnetics Research*, Vol. 94, 351–366, 2009.
14. Qiu, C. W., N. Burokur, S. Zouhdi, and L. W. Li, "Chiral nihility effects on energy flow in chiral materials," *J. Opt. Soc. Am. A*, Vol. 25, No. 1, 55–63, 2008.
15. Tuz, V. R. and C. W. Qiu, "Semi-infinite chiral nihility photonics: Parametric dependence, wave tunneling and rejection," *Progress In Electromagnetics Research*, Vol. 103, 139–152, 2010.
16. Dong, J. F., "Surface wave modes in chiral negative refraction grounded slab waveguides," *Progress In Electromagnetics Research*, Vol. 95, 153–166, 2009.
17. Faryad, M. and Q. A. Naqvi, "High frequency expression for the field in the caustic region of cylindrical reflector placed in chiral medium," *Progress In Electromagnetics Research*, Vol. 76, 153–182, 2007.
18. Faryad, M. and Q. A. Naqvi, "Cylindrical reflector in chiral medium supporting simultaneously positive phase velocity and negative phase velocity," *Journal of Electromagnetic Waves and Applications*, Vol. 22, No. 4, 563–572, 2008.
19. Ghaffar, A., Q. A. Naqvi, and K. Hongo, "Analysis of the fields in three dimensional Cassegrain system," *Progress In Electromagnetics Research*, Vol. 72, 215–240, 2007.